electricity

MDPI

Article

A Methodology for Testing the Size and the Location of Battery Energy Storage Systems on Transmission Grids

Nicola Collura [1,*], Fabio Massaro [1], Enrica Di Mambro [2], Salvatore Paradiso [2] and Francesco Montana [1]

1 Department of Engineering, University of Palermo, Viale delle Scienze Building 9, 90128 Palermo, Italy; francesco.montana@unipa.it (F.M.)
2 Terna S.p.A, Viale Egidio Galbani, 70, 00156 Rome, Italy
* Correspondence: nicola.collura@unipa.it; Tel.: +39-3204410882

Abstract

A replicable methodology for testing the size and placement of Battery Energy Storage Systems connected to high-voltage transmission networks is presented in this study. The proposed approach involves the power flow analysis inside a Renewable Energy Zone, namely a high-renewable area prone to grid congestion during peak generation periods, based on time-series hourly analysis over a critical month. The model includes detailed operational descriptions such as lines ampacity, battery state of charge limits, round-trip efficiency, self-discharge behavior, and ramp rate restrictions. The methodology distinguishes itself by its simplicity, flexibility, and use of open-source tools, making it a valuable asset for supporting future transmission planning in high-renewable-energy scenarios. The model was developed in Python (version 3.12) using the open-source Pandapower library, introducing an innovative constraint management criterion, and validated against real data provided by the national Transmission System Operator. The approach was then applied to a portion of the Sicilian grid with massive wind and solar penetration. Results show that strategic allocation of batteries leads to a significant reduction in line overloads (up to 13 GWh mitigated in one month), improves the dispatch of renewable energy generated within the Renewable Energy Zone and allows a more sustainable exercise of the power system.

Keywords: congestion; energy storage; optimal power flow; renewable energy; transmission

1. Introduction

Producing electricity from Renewable Energy Sources (RES) is fundamental to decarbonizing the energy sector and meeting international agreements on global warming mitigation strategies. Although wind and solar energy sources are the most abundant RES, they have the critical drawback of being intermittent sources. These large-scale storage systems, characterized by large storage capacity and high-power rating, will enable more effective integration of RES through time-shifting services, improving system adequacy and helping to resolve grid congestion. This aspect provokes intrinsic uncertainty in electricity production, which challenges the proper operation of power grids, especially transmission grids managed by Transmission System Operators (TSOs). Among these challenges is certainly the resolution of grid congestion, typically occurring during the middle hours of the day due to the peak solar production. For instance, the transmission network of Sicily, the largest island in the Mediterranean Sea area, which currently hosts about 4.5 GWp of installed renewable capacity [1–3], is expected to integrate additional 9.4 GWp of cumulated

Check for updates

Academic Editors: Andreas Sumper, Ottorino Veneri and Emilio Gomez-Lazaro

Received: 22 January 2026
Revised: 5 March 2026
Accepted: 26 March 2026
Published: 4 April 2026

RES plants, as established by the Italian 2030 Integrated National Energy and Climate Plan (in Italian, *Piano Nazionale Integrato per l'Energia e il Clima* or PNIEC) [4].

To address this scenario, Terna S.p.A., the Italian TSO, draws up and periodically updates a grid development plan to improve the electricity infrastructure in order to ensure safe and efficient network operating conditions [5]. Among the measures adopted, Terna introduced the subdivision of the national territory into so-called *micro-zones*, allowing for simplified modeling and control of energy flows across the grid. When a micro-zone hosts a significant concentration of renewable plants, it is defined as a *Renewable Energy Zone* (REZ): a portion of the network which behaves like an equivalent power generator [6,7]. Since REZs are particularly prone to congestions, especially when local generation exceeds the export capacity of transmission lines, the safe operation of REZs requires the improvement in its flexibility, namely the ability of the power system to cope with variability and uncertainty introduced by demand and generation from non-programmable renewable sources. A flexible power system is able to supply all the energy required by consumers, minimizing system costs [8,9]. An effective technique to improve grid flexibility is to resort to storage systems, which allow electrical energy to be stored during production peak hours and returned during demand peak hours. For instance, with reference to solar energy, it might be stored in the middle of the day and released at times when the power grid is not overloaded.

The development planning of modern power grids involves several aspects, mainly on the current meshing of the local grid, and the current and programmed location of solar and wind plants, but should also involve the correct sizing and optimal siting of storage systems to properly manage local congestions, wherever necessary. Electrochemical storage systems, commonly referred to as Battery Energy Storage Systems (BESS), are currently among the most important energy storage technologies in high-voltage systems [10–12], together with large pumped-hydro power plants.

To promote the integration of BESS into the electricity market, the Italian energy authority, ARERA, together with the TSO, promoted an innovative long-term contracting mechanism: the *Electric Storage Capacity Procurement Mechanism* (in Italian, *Meccanismo di Approvvigionamento di Capacità di Stoccaggio Elettrico* or MACSE), which was launched on 2025 [13]. According to the *Scenarios Description Document* (DDS24) issued by Terna [14], a total storage capacity of 71.5 GWh will be installed and connected to the national transmission grid over the next ten years, mainly in southern Italy and the major islands. In Sicily, according to the PNIEC 2030 scenario, large-scale electrochemical storage systems will be connected to the grid for a total capacity of 14.4 GWh.

An efficient utilization of storage systems also allows the reduction in CO_2 emissions, since they can substitute traditional power plants suppling energy during the hours of low renewable energy production. They will also be able to provide ancillary services such as voltage regulation, inertia emulation, and short-circuit support [8,15]. Although the sizing and siting of BESS in HV power systems is timely, only a few studies on this topic are available in the international scientific literature.

In [16], a multi-objective optimization model is presented, implemented in MATLAB (R2021a, version 9.10), which enables the sizing of energy storage systems connected to a portion of the transmission network. The study, based on economic and energy curtailment minimization, shows that a hydrogen-based storage should be preferred to BESS technology.

In [17], operational benefits of BESS deployment in a transmission network are highlighted, implementing the model on Pandapower library [18–20]; in this paper, a three-bus ring system is studied by emphasizing the dynamic interaction between generation with renewable energy, consumption, and storage, demonstrating how advanced battery management can enhance grid stability and efficiency. In [21], a case study is described for a hybrid solar–BESS system for a microgrid or local load. In this paper, the role of BESS in frequency dynamic support and managing have been studied. The results show that such fast-acting storage technology like BESS can help to maintain system stability as impacted by penetration of RESS generation in the case of a major generation outage. In [22], the Pandapower library is used to evaluate the operation of storage systems connected to the transmission grid, and a detailed assessment is made of the importance of various aspects in the sizing and siting of BESSs. In [23], a time series optimization-based method for optimizing reactive power provision through Pandapower is proposed. The study shows that appropriate control characteristic curves for distributed energy sources support stable and efficient distribution grid operation.

In [24], the optimization of grid topology for a distributed electrical system with renewable energy penetration is described. Thanks to Pandapower tools, the optimal topology to minimize energy losses have been determined. The analysis of the existing literature shows a lack of proper description of the local power grid or the coupling between optimization systems and power flow analysis. Moreover, in the whole literature analyzed, the validation of methods due to lack of technical data that only TSOs can provide is not evident.

In order to overcome this highlighted research gap, the main purpose of this article is to provide a methodology for testing the size and the location of storage systems connected to a portion of the transmission grid. The authors developed an innovative technique to manage the optimal power flow of REZs including BESSs. The adoption of the methodology developed for this study allows for assessing whether the size, ramp, nominal power, and siting of a storage system are effective in mitigating grid congestion caused by high production from renewable energy sources.

The simulation model was developed on Pandapower (PP) open-source library, enhancing the accessibility of the method. The application of this study focuses on the BESS units connected to a portion of the Sicilian transmission grid identified as a REZ.

The collaboration with the Italian TSO allowed using technical data and tools not typically available in academic settings. This allowed the modeling of the transmission grid of a Sicilian REZ, with the support of free tools accessible to everyone.

2. Methodology

This section outlines the methodology adopted to implement the network in the Python environment, perform optimal power flow (OPF) time-series simulations, and obtain the study results. The methodology presented stands out for its originality, ease of implementation, and use of an innovative approach: the optimization algorithm is based on a characteristic feature of areas with high penetration of renewable sources: these areas behave as equivalent generators for the rest of the electrical system. Therefore, thanks to a free and open-source tool such as Pandapower, it is possible to exploit this logic to optimize the operation of storage systems. From a purely energy-related and non-economic point of view, they should only be used when it is the only option to avoid grid congestion. Therefore, the study stands out for choosing this approach, which has not been adopted in the literature. The authors highlight that the time-series analysis is carried out with a time resolution of one hour under the assumption that energy flows remain constant within each time step. For this reason, all the PP functions and the optimal power flow time-step results can be expressed in MWh, even if they were set as power by defaults.

2.1. Development of the Transmission Network Model

The methodology begins with the implementation of the transmission network in the Python environment. The open-source library Pandapower (PP) was used, and the PP functions in Table 1 are applied to create the network model.

Table 1. Pandapower functions used to create the network model.

Function	Description
create_empty_network	Creates the empty network to which all the elements can be added
create_bus	Defines all the buses of the grid
create_line_from_parameters	Defines each transmission line and its parameters
create_trafo	Defines each transformer and its parameters
create_sgen	Models each generation plant
create_load	Models each electrical load
create_gen	Defines each external grid
create_storage	Defines each storage system and its parameters

Once the grid elements have been modeled, it is necessary to assign generation profiles to the energy plants and the load profiles to the loads. The proposed methodology employs hourly average values to populate the profiles. This choice was based on the assumption that profiles usually remain constant for over an hour or can vary only slightly. This hypothesis is considered plausible because the study does not focus on analyzing the dynamic behavior of the network and BESSs, which can experience sudden fluctuations in energy transmission in a matter of seconds, but rather on its average behavior during each day. Furthermore, the technical features of the BESS used by Terna S.p.A. and already available on the market are such that they can easily manage any sudden load variations [25]. Furthermore, adopting hourly resolution allows for the analysis of extended time periods of time while avoiding excessive computational overhead. Table 2 contains the functions needed to associate the profiles.

Table 2. Pandapower functions used to fill the profiles.

Function	Description
net.sgen[“controllable”] = True	Each generation plant can be associated with its generation profile through extraction file
net.load[“controllable”] = True	Each load can be associated with its load profile through extraction file
pandas.read_excel	Excel files can be used as extraction file for generation and load profiles
pandas.DataFrame	Columns in pandas.DataFrame can be created to contain generation or load profiles
ConstControl	Allows to associate each time-step DataFrame with the corresponding grid element

2.2. Storage Systems Constrains

The second aspect of the methodology concerns the implementation of the time-series analysis. It is important to note that the function for time-series analysis already exists in the PP library, but this function does not take into account the evolution over time of the state of charge (SOC) of the various storage systems, nor their characteristic ramp rates. Neither the self-discharge rate nor the charging and discharging efficiency of the storage systems are considered. In detail, here are the equations that represent these necessary constraints implemented in Python environment, which allow for more accurate time-series analysis:

$$C_{ij} = C_{ij-1} \cdot (1 - \lambda_{sd}) + E_{ij} \cdot \eta_{ch},\ E_{ij} > 0 \quad (1)$$

$$C_{ij} = C_{ij-1} \cdot (1 - \lambda_{sd}) + E_{ij}/\eta_{disc},\ E_{ij} < 0 \quad (2)$$

Here is the description of Equations (1) and (2): C_{ij} is the energy stored in the *i*-th storage system after hour *j* [MWh], C_{ij-1} is the energy stored in the *i*-th storage system after hour $j - 1$ [MWh], E_{ij} is the energy absorbed (positive) or released (negative) by the *i*-th storage system during hour *j* [MWh], λ_{sd} is the self-discharge rate of the storage system [dimensionless], η_{ch} is the charging efficiency of the BESS [dimensionless], and η_{disch} is the discharging efficiency of the storage system [dimensionless]. The state of charge SOC_{ij} of each storage system is calculated through the fallowing equation:

$$SOC_{ij} = 100 \cdot C_{ij}/C_{max,i}\ [\%] \quad (3)$$

where C_{ij} is the energy stored in the i-th storage system after hour *j* [MWh] and $C_{max,i}$ is the nominal capacity of the i-th storage system [MWh]. The state of charge SOC_{ij} depends on the energy absorbed/supplied by the BESS in the previous hour according to Equation (3). Equation (4) is used to calculate the hourly charge limit of each BESS, which takes into account the energy accumulated by the BESS up to that point via $C_{max,i} - C_{ij}$, the technological limit of the BESS via $E_{max,i}$, and the maximum ramp rate of the BESS via R_{ij}:

$$E_{max,ij} = min(C_{max,i} - C_{ij-1},\ E_{max,i},\ R_{ij}) \quad (4)$$

where R_{ij} is the ramp rate that the BESS can sustain during charging, which is calculated according to Equation (5):

$$R_{ij} = E_{ij-1} + R_{max} \quad (5)$$

In this equation, R_{max} is the maximum charge/discharge rate that the i-th storage system can sustain within one hour [MWh], R_{ij} is the maximum ramp rate that the i-th storage 4 system can sustain within hour *j* [MWh], E_{ij-1} is the energy absorbed/supplied by the i-th storage system in the previous hour [MWh]. Equation (6) is used to calculate the hourly discharge limit of each BESS. It takes into account the energy accumulated by the BESS up to that point via $-C_{ij}$, the technological limit of the BESS via $E_{max,i,}$ and the maximum ramp rate of the BESS via R_{ij}:

$$E_{min,ij} = max(-C_{ij-1},\ -E_{max,i},\ R_{ij}) \quad (6)$$

where R_{ij} is the ramp rate that the BESS can sustain during discharging, which is calculated according to the Equation (7):

$$R_{ij} = E_{ij-1} - R_{max} \quad (7)$$

In this equation, R_{max} is the maximum charge/discharge rate that the i-th storage system can sustain within one hour [MWh], R_{ij} is the maximum ramp rate that the i-th storage system can sustain within hour *j* [MWh], and $E_{i,j-1}$ is the energy absorbed/supplied by the i-th storage system in the previous hour [MWh]. C_{ij-1} is the energy stored in the i-th storage system after hour $j - 1$ [MWh] and $C_{max,i}$ is the nominal capacity of the i-th storage system [MWh].

Equations (4) and (6) show other operating constraints implemented on PP: each BESS can only absorb energy or feed it into the grid in compliance with these equations. In Equation (6), the minimum energy that can be supplied by each storage system *i* for each hourly step *j* is calculated. This can only be the smallest value (close to zero, negative) among the amount of energy accumulated by the storage system, the maximum amount of energy that can be supplied based on the storage system's construction characteristics, and the maximum ramp rate that the storage unit can sustain based on its characteristics.

Equation (4) is used to calculate the maximum energy that each storage system can absorb each time step with the same criteria. So these are the parameters of the model that must be defined to perform each simulation: $E_{max,i}$, $C_{max,i}$, $SOC_{i,0}$ (that is the starting SOC of the i-th BESS), η_{ch}, η_{disch}, λ_{sd}, R_{max}.

To limit battery degradation, it is always advisable to maintain the SOC of each BESS between 20% and 80% of its nominal storage capacity. In this methodology, this constraint is not considered during the process but only at the end. Therefore, if a $C_{max,i}$ of 200 MWh for each storage facility was proposed as input for the model, in order to keep the SOC within the permitted limits, a real $C_{max,i}$ equal to 330 MWh would be necessary.

2.3. Bounds of the Optimal Power Flow

Once the network model has been implemented and the operational constraints of storage systems introduced into the model for time-series analysis have been explained, the bounds imposed on the variables through PP library are shown in Table 3.

Table 3. Pandapower functions used set operation constrains.

Function	Description
net.line["max_loading_percent"] = 100	Allows to set loading limit of each transmission line equal to his ampacity [%]
net.gen.loc[i-th external grid, "min_p_mw"] = Numerical Value	Allows to set the nominal import capacity of the external grids (active power, MWh)
net.gen.loc[i-th external grid, "max_p_mw"] = Numerical Value	Allows to set nominal export capacity of the external grids (active power, MWh)
net.gen.loc[i-th external grid, "min_q_mvar"] = Numerical Value	Allows to set the nominal capacity of the external grids (reactive power, MVARh)
net.gen.loc[i-th external grid, "max_q_mvar"] = Numerical Value	Allows to set the nominal import capacity of the external grids (reactive power, MVARh)
net.storage.loc[i-th storage system, "max_q_mvar"] = Numerical Value	Allows to set the maximum reactive energy that the i-th storage system can absorb in each time-step (MVARh)
net.storage.loc[i-th storage system, "min_q_mvar"] = Numerical Value"	Allows to set the maximum reactive energy that the i-th storage system can release in each time-step (MVARh)
net.storage.loc[i-th storage system, "max_p_mw"] = Emax,ij	Allows to set maximum active energy that the i-th storage system can absorb in each time-step (MWh, Equation (3));
net.storage.loc[i-th storage system, "min_p_mw"] = Emin,ij	Allows to set the maximum active energy that the i-th storage system can release in each time-step [MWh] (Equation (5))
net.bus["min_vm_pu"] = 0.98	Allows to set the minimum voltage level for each bus of the network [%]
net.bus["max_vm_pu"] = 1.02	Allows to set the maximum voltage level for each bus of the network [%]
net.trafo["max_loading_percent"] = 110	Allows to set loading limit of each transformer equal to his nominal rate (%).

https://doi.org/10.3390/electricity7020035

As can be seen, the PP library defines the bounds relating to external networks and storage systems in terms of power rather than energy. However, in the proposed methodology, analyses are carried out with a time resolution of one hour under the assumption that energy flows remain constant within each time step. For this reason, the numerical values imposed in each bound can be indicated as energy, expressed in MWh. An important aspect to highlight is that almost all these bounds are defined only once and remain constant for all time-steps. The bounds relating to the active power that each storage unit can absorb or release are variable and must be updated after each simulation, because they must take into account Equation (4) during charging and Equation (6) during discharging. Furthermore, it should be noted that in this methodology, we decided to disregard the analysis of reactive energy flows. The impact of explicitly modeling reactive power flows and voltage constraints expected would be not so relevant, because Terna has implemented many compensators and shunt reactors along all the transmission grid, meaning that this issue has been neglected. For this reason, the limits relating to the reactive energy of loads, generators, storage systems, and external grids were imposed to ensure the simulation of each OPF but are not relevant.

2.4. The Objective Function

In addition to the bounds, the Pandapower library allows setting objective functions such as cost functions. In this methodology, the "maximization of energy export through external networks" can be imposed as an objective function. The reason for this choice is that the modeled transmission network was assumed to be a REZ and, since REZs typically export energy to meet the needs of the network, the TSO's objective is usually to maximize energy production within the REZ and export it from there.

In Python, the command that must be applied to each external grid to implement this objective function is as follows: "pp.create_poly_cost(net, i-th external grid, "gen", cp1_eur_per_mw = 1)".

Imposing this cost function ensures that any storage systems connected to the network only absorb energy when strictly necessary in order to comply with constraints and bounds. For example, when production from renewable sources in the REZ is high enough to overload the transmission lines, BESSs are activated to prevent this from happening. Storage systems do not absorb energy in other cases because the charging operation of BESS would reduce the export of energy from the REZ to external grids, which is perceived as a cost to be minimized by PP's OPF algorithm. Conversely, when the BESSs are charged and the transmission network is not saturated, the BESSs are automatically discharged, maximizing the objective function, i.e., the export of energy to external networks.

Therefore, the decision to maximize energy export effectively allows the main aim for which BESSs are implemented in the grid to be achieved, namely resolving grid congestion. This is because, regardless of the cost function implemented, the priority of the optimization algorithm is to comply with the constraints imposed (the ampacity of each power line) in the load flow calculation.

It should be noted that the load status of power lines is constantly monitored by the network operator through TA current transformers interfaced to Terna system control, so this methodology could be technically and theoretically applicable in the daily operation of the transmission network.

2.5. Handling of OPF Non-Convergence

When the OPF function is run, a solution may not be found. There are two possible reasons for this: actual absence of OPF solutions that comply with the imposed bounds and divergence of the numerical method within the algorithm. This possibility may occur as indicated on the PP library website [18].

This subsection explains the strategy adopted to establish the causes of non-convergence in the OPF function. The free variables that the OPF function uses to find the solution are as follows: energy absorbed/released by external grids in each time-step; energy absorbed/released by storage systems (if they are present) in each time-step.

When the OPF does not converge, an initial power flow (PF) is performed to determine the cause of the OPF no-convergence. To run the function, the command "run.pp" from the Pandapower library is used. In this PF, the free variables listed above are transformed into fixed parameters. The storage systems are connected to the network without supplying energy thanks to the following command in Python: "net.storage.loc[i-th storage system, "in_service"] = False".

Since the power flows affecting the external grids should not vary greatly from one hour to the next, it was decided to impose the energy flows from the $j-1$ time-step on the external grids so that it is equal to the energy flows in the j time-step. Equation (8) describes the above:

$$EG_{ij} = EG_{ij-1} \tag{8}$$

where EG_{ij} is the energy flow through the i-th external grid in the j time-step [MWh] and EG_{ij-1} is the energy flow through the i-th external grid in the $j-1$ time-step [MWh].

It is the slack bus that compensates for any differences between generation and loads in power flow analysis. In this study, a distributed slack configuration was imposed across all external grids. This choice keeps the network balanced.

If the PF results show that power lines and transformers are not loaded beyond 100%, this demonstrates that the OPF cannot find a solution due to the divergence of the internal algorithm, even though at least one solution actually exists.

In this case, the BESSs were not used improperly because they are connected to the grid but do not supply or absorb energy. Therefore, although an optimal solution that minimizes the cost functions was not found, the PF results are saved for the time step and the SOC of the BESSs remains constant, apart from self-discharge losses.

If, on the other hand, at least one of the power lines or a transformer has become overloaded as a result of the PF, a very simple iterative method is applied in which all BESSs are required to participate by absorbing energy at the PF.

Through a for loop, the BESSs connected to the grid (if present) are required to absorb a certain amount of energy, in compliance with the constraints seen previously, according to Equations (5) and (9):

$$E_{ij} = min(C_{max,i} - C_{ij-1}, E_{max,i}, R_{ij}) \cdot C \tag{9}$$

In Equation (9), C_{ij-1} is the energy stored in the i-th storage system in the $j-1$ time-step [MWh], $C_{max,i}$ is the nominal capacity of the i-th storage system [MWh], E_{ij} is the energy absorbed by the i-th 7 storage system in the j time-step [MWh], $E_{max,i}$ is the charge limit of the i-th BESS in the j time-step [MWh], C is the modulation coefficient of the energy absorbed by all BESSs [dimensionless], and R_{ij} is the ramp rate that the i-th BESS can sustain in the j time-step.

The modulation coefficient C of the energy supplied by each storage system is gradually varied from 0 to 1 in increments of $1/10$ through a for loop. A PF is run for each step of the iterative method. As soon as the load limits of lines and transformers are met, the for loop is interrupted, the results are saved, and the next step is performed.

Technically, the OPF function should resolve these cases, and in most cases it does. Nevertheless, in some cases, the proposed iterative method becomes essential, and although it is not an OPF, the solution found is still close to optimal. It should also be noted that in subsequent iterations, which normally converge, those BESSs that were used even though it was not extremely necessary will discharge the energy stored in the previous step, thanks to the chosen objective function.

If even the last iteration does not mitigate the grid congestion, it is a real and unavoidable congestion caused by at least one power line or transformer. This situation occurs mainly when BESS have been absorbing energy for several hours in a row and are saturated at the time when congestion occurs. This can also occur because the energy required to mitigate the grid congestion exceeds the technical limit of the BESS imposed as a constraint, although the BESSs are not saturated (Equation (9)). Figure 1 shows a summary of the algorithm explained so far.

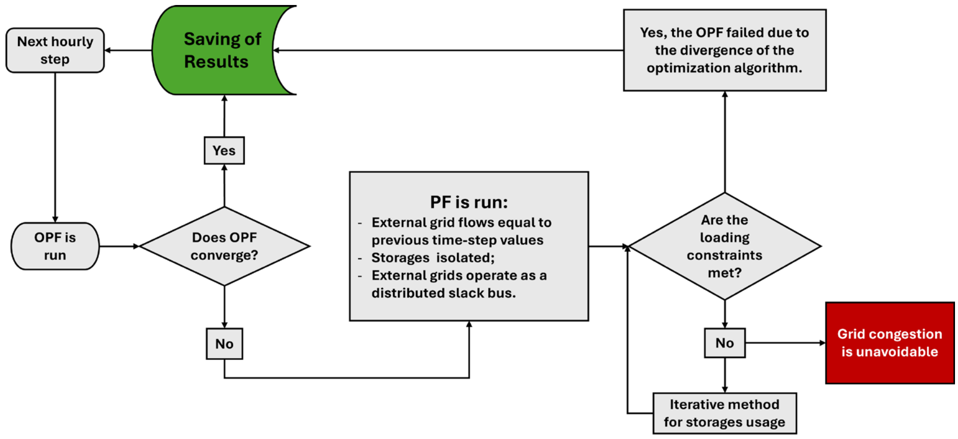

Figure 1. Algorithm flowchart.

2.6. Result Analysis

The final part of the methodology concerns the analysis of the results obtained. It should be noted that the main purpose of the simulations is to assess whether it is useful to install storage systems in the transmission network to avoid grid congestion. Therefore, the most important simulation results to be analyzed are (i) the loading level of power lines over time compared to their ampacity; (ii) the loading level of transformers over time compared to their rated capacity; (iii) the state of charge of storage systems over time; and (iv) energy absorbed or released by storage systems over time.

The PP library in Python makes it possible to easily track this data hour by hour, which can be viewed using graphs or saved as text files.

Analyzing lines and transformers' loading level permits assessing whether the grid is sufficiently robust, to identify power lines that limit the efficiency of the REZ, and whether any transformers need to be replaced. The loading level of lines and transformers also depends on the effectiveness of the modeled storage systems.

Evaluating the SOC of storage systems makes it possible to understand whether each storage system has been sized effectively and to evaluate its usefulness relative to the others. The optimization algorithm will always try to operate storage systems in the most efficient way, i.e., to export as much energy as possible from the REZ. Therefore, the operation of each storage system may differ, and those storage systems that are used most frequently play a more important role in the network.

In the event of overloads, it is useful to calculate the amount of energy causing grid congestion. Calculating this amount of energy may not be immediate or easy. The main aspect to consider is the positioning of the lines that are overloaded in the network.

If overloaded power lines are close together and therefore connected in series with each other, the energy flows through one line could be the same, entirely or in part, as those

https://doi.org/10.3390/electricity7020035

through the nearby overloaded power lines. Conversely, if the overloaded power lines are far apart, the energy flows through them can be considered independent.

In order to correctly calculate the amount of energy responsible for grid congestion, it is therefore necessary to study the transmission network on a case-by-case basis, performing a sensitivity analysis of the power lines loading. Once the overloaded power lines responsible for grid congestion have been identified, it is possible to quantify the amount of energy causing line overloading through Equation (10), where the line overloading LO_i of the single line i was calculated for all hours m of the period chosen for the simulations. Equation (11) was used to calculate the total overload of the lines LO_{tot} for all the m hours of the period chosen for the simulations.

$$LO_i = \sum^m max(LC_{ij} - LC_i, 0) \tag{10}$$

$$LO_{tot} = \sum^m \sum^n max(LC_{ij} - LC_i, 0) \tag{11}$$

where LC_{ij} is the energy carried by the i-th overloaded line during j time-step [MWh]. LC_i is the hourly capacity of i-th line [MWh]. LC_i has been calculated by multiplying the ampacity of the line (MW) of the time-step duration (one hour). $LC_{ij} - LC_i$ is the amount of energy causing i-th line overloading in j time-step [MWh], and $\sum max(LC_{ij} - LC_i, 0)$ is the total amount of energy causing n line overloading in j time-step.

Based on the values of LO_i and LO_{tot}, it is possible to determine which lines are most important for the transmission network. It is possible to determine which lines constitute the bottleneck of the transmission network. These lines, for example, could be improved or replaced with lines with greater ampacity [26]. Alternatively, low-cost, targeted interventions could be carried out using Dynamic Thermal Rating [6]. Combining different solutions and repeating the simulations would allow for further optimization of the use of storage systems.

3. Model Validation

To validate the methodology, a portion of the transmission network in northwestern Sicily, which can be considered a Renewable Energy Zone, was modeled. This REZ includes three 220 kV electrical stations and two 150 kV electrical stations, as well as generation plants and loads. The 150 kV stations are connected to the 220 kV stations through transformers with a rated power of 250 MVA or 160 MVA.

The power lines were modeled using the Pandapower library. It is important to collect the most important characteristics of lines in order to model them correctly: line length, capacity, reactance, resistance, inductance, ampacity, and voltage level. The same reasoning applies to the transformers implemented, which were appropriately sized. Other topological elements intended for changing the network configuration (switches, disconnectors, TVs, and TAs) were not modeled, as the standard operating topology was taken into consideration.

The transmission network studied is interconnected with the external transmission network through six power lines named as external grids. These connections have been modeled as controlled generators capable of both supplying electricity to the network and absorbing the energy flows produced in it. Their ampacity has been considered. The 220 kV external grids ampacity is about 900 A, while the 150 kV external grids ampacity is approximately 700 A. Each external grid participates as distributed slack bus in equal measure when normal power flows are run. The generation plants and loads are connected via one of the two bus-bars that make up each station. All 26 loads and all 22 generation plants connected to the transmission grid have been modeled.

https://doi.org/10.3390/electricity7020035

It is crucial to model power lines and elements with their actual characteristics, but this is usually quite difficult in academia since this data is held by TSOs. Many studies highlight this limitation, as in [22]. The availability of this data made it possible not only to develop a methodology but also to apply it concretely to a case study, fully adhering to the reality being modeled. Figure 2 shows the transmission network studied as implemented on PP.

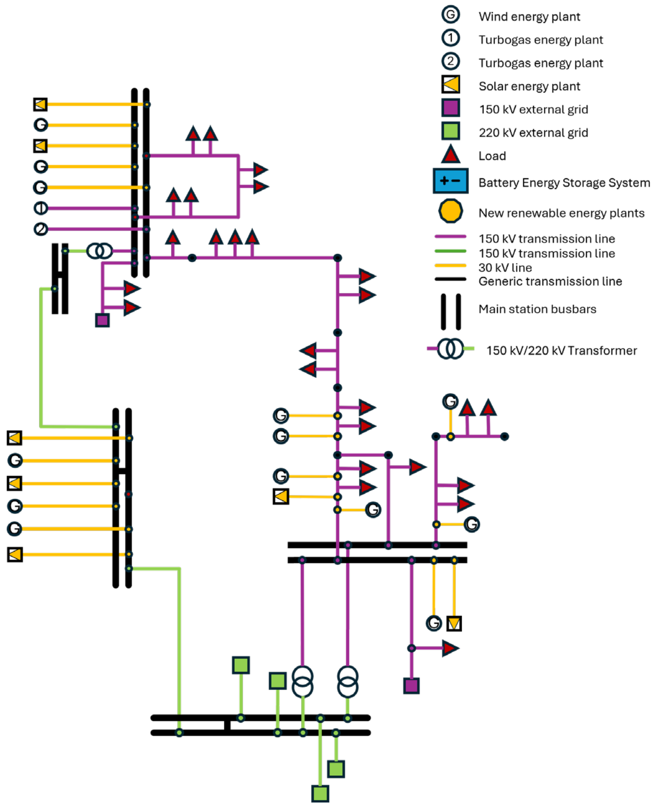

Figure 2. Transmission grid of the REZ modeled in Python.

Once the REZ topology has been modeled, the generation profiles of the 22 plants and load profiles of the 26 loads have been collected through TSO's databases. Terna S.p.A. uses a software called "Terna Data Viewer" (TDV, version 3.7.5) to record the electricity flows circulating on all transmission lines, the energy flows produced by generation plants, and the energy flows absorbed by loads.

In order to validate the current network model implemented on PP and to verify that the network topology adopted is correct, we decided to simulate the operation of the network during the month of July 2024. Figure 3 shows the total hourly energy exchange between the REZ and the rest of the Sicilian transmission grid, through the six external grids according to TDV measurements. In this figure, positive flows indicate that the grid absorbs energy from outside, while negative flows indicate that the grid exports energy to the outside.

Figure 4 shows the total hourly energy exchange between REZ and the rest of the Sicilian transmission network, through the six external grids, according to simulations carried out with PP. In this figure, positive flows indicate that the network absorbs energy from outside, while negative flows indicate that the network exports energy to the outside.As shown in Figures 3 and 4, only minor differences are observed. One possible reason for the differences between the simulations and measurements is that the telemetry measurements used and implemented in TDV are indicative but not always accurate, due to the normal inaccuracy of measuring instruments.

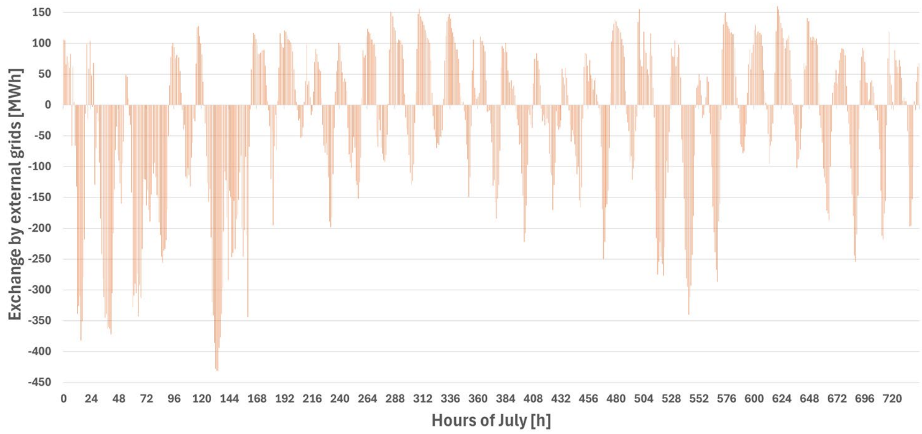

Figure 3. Total hourly energy exchange between the REZ and the external grids according to TDV.

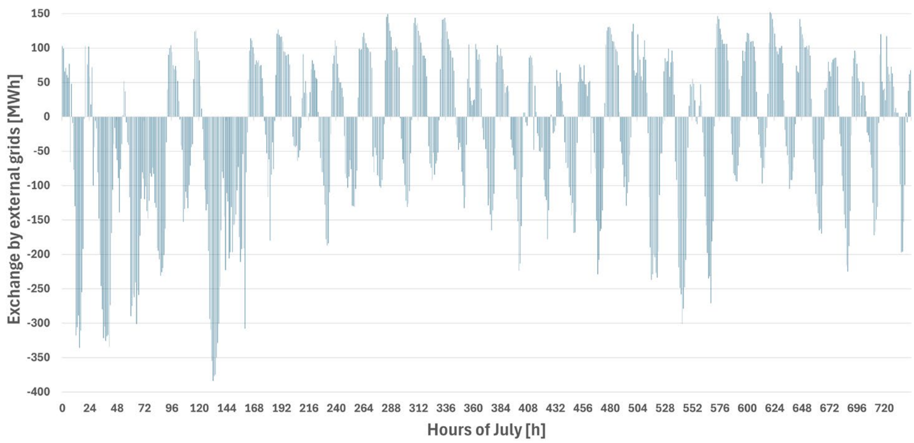

Figure 4. Total hourly energy exchange between the REZ and the external grids according to PP.

A numerical indicator, shown in Equation (12), quantifies the degree of correspondence between the simulations and the telemetry measurements. It is the average hourly deviation between the simulated exchange with the external network and the exchange with the external network measured by the TDV. The average is calculated by dividing by the total number of hours in July (744 h).

$$D = \sum_{1}^{743} | Ex_{PP,j} - Ex_{TDV,j} | /744 \quad (12)$$

where $Ex_{PP,j}$ is the total energy exchange between the REZ and external grids in hour j according to simulations on PP [MWh], and $Ex_{TDV,j}$ is the total energy exchange between the REZ and external grids in hour j according to TDV measurements [MWh].

The D value obtained is equal to 14 MWh. This result is considered satisfactory, given that an average of 300–400 MWh of electricity circulates within the REZ every hour. Based on the results obtained, the network has been correctly modeled in the Python environment and that the OPF logic used by the library is consistent with that used in practice by the Italian TSO.

Additional statistical indicators have not been evaluated because the aim was not to test pandapower functions, but to ensure the correctness of the transmission grid topology and characteristics implemented. Therefore, parameter D should be sufficient. Furthermore, comparing actual energy flows within the network with simulated ones may not be useful, as maintenance operations and topological changes that occur on a daily basis often cannot be simulated.

4. Case Study

The purpose of this section is to illustrate the application of the methodology previously described to a real case study. As highlighted in the introduction, Sicily will need to integrate a large amount of renewable energy in the coming years. The REZ modeled on PP in Figure 2, located in the western part of the region, will also have to accommodate new wind and solar plants according to studies [6,16,27].

The methodology allows for simulations of REZ operation, to which the future generation from renewable sources expected in the area is added [28]. According to Terna sources, by 2030 the REZ should accommodate at least 1.2 GW of new wind and solar power plants.

Storage systems could be crucial in mitigating grid congestion; therefore, in this case study, a comparison was made between future network operation with storage systems and without storage systems.

It is difficult to predict exactly which network buses will be chosen to connect new energy plants. For this reason, the future generation was added to the network the way shown in Figure 2 to avoid this obstacle. The planned plants were connected directly to certain REZ stations, allocating 400 MW of future power installed to each of the three stations. At each selected station, half of the planned future plants were connected to one bus-bar and half to the other bus-bar. The total future power installed is about 1.2 GW (0.6 GW of solar plants and 0.6 GW of wind plants). In addition to the expected future generation, six storage systems have been added to the network shown in Figure 2, which are also evenly distributed throughout the REZ using the same criteria. Figure 5 shows what has been described so far.

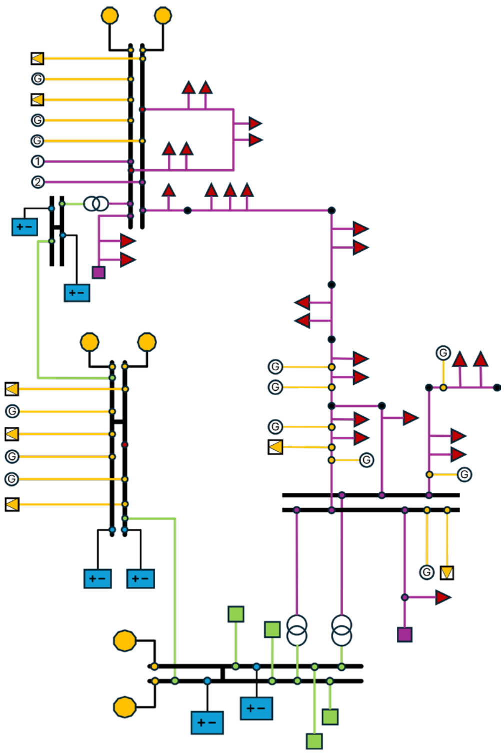

Figure 5. Transmission network of the REZ with future generation and storage systems.

In order to carry out the case study simulations, it was necessary to choose the period of time to be analyzed. The time period chosen for the simulations is a typical summer month such as July. Therefore, the load profiles for each load are those used for model validation, as they refer to the month of July 2024. The generation profiles of the plants currently present in the REZ are also the same profiles used in the model validation.

4.1. Future Generation Plants Profiles

The generation profiles of these plants should comply with their typical technology characteristics and be consistent with the solar irradiance and wind conditions of the area. To get these profiles, the productivity data of existing solar and wind power plants in the area were used and applied to the expected future generation. Equation (13) is how the hourly producibility values to be applied to future generation were calculated:

$$P_{ij} = 100\cdot G_{ij}/G_{max,i}\ [\%] \quad (13)$$

Here is the description of Equation (13): P_{ij} is the producibility of i-th future wind or solar generation plant in hour j [%], G_{ij} is the energy produced by the reference solar or wind plant i in hour j according to TDV measurements [MWh], $G_{max,i}$ is the maximum amount of energy that the reference solar or wind power plant i can produce based on its rated power [MWh]. Using TDV software (version 3.7.5), the generation profiles of a reference wind farm in the area during July 2024 and the generation profile of a reference solar plant in the area during the same period were extracted. Figures 6 and 7 show the selected profiles. In the figures, the y-axis shows the percentage of actual power produced power compared with the nominal power of the plants

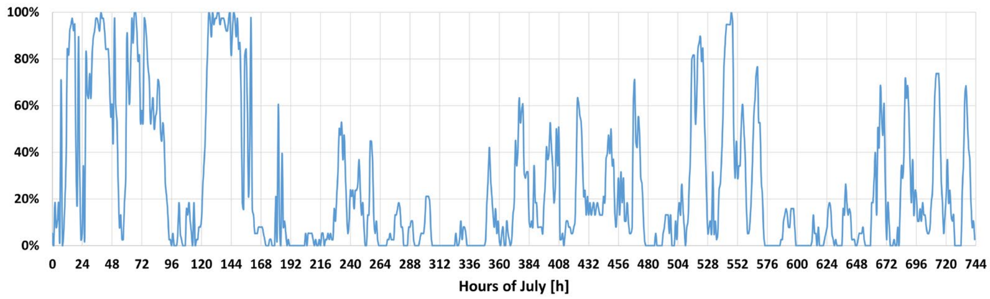

Figure 6. Typical generation profile of wind plants inside the REZ in July.

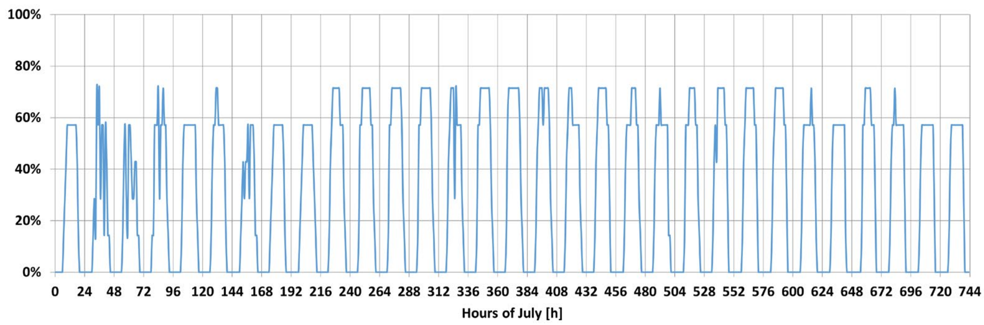

Figure 7. Typical generation profile of solar plants inside the REZ in July.

4.2. Selection of Storage Systems Features

In order to perform the simulations, it is necessary to select the characteristic parameters of the storage systems. In the work carried out, the same characteristics were chosen for all six storage systems. Table 4 shows the selected parameters. These parameters are consistent with the state of the art in electrochemical storage technologies suitable for connection to the transmission network [1,10].

The value of $C_{max,i}$ chosen corresponds to 330 MWh when considering the charging limit (below 80%) and discharging limit (above 20%) required to preserve battery lifetime [29,30]. The decision of not explicitly enforcing the 20–80% SOC operational limits within the OPF formulation has no impact on the dispatch behavior if the actual nominal capacity of each BESS chosen is 330 MWh. It is possible because the lower bound of OPF

(0 MWh) corresponds to the actual value of SOC equal to 66 MWh (20% of 330 MWh) and the upper bound of OPF (200 MWh) corresponds to 266 MWh (80% of 330 MWh).

Table 4. Parameters used to describe storage systems.

Parameter	Value
$E_{max,i}$	50 MWh
$C_{max,i}$	200 MWh
$SOC_{i,0}$	0%
η_{ch}	0.92
η_{disch}	0.92
λ_{sd}	0.002
R_{max}	100 MWh

5. Results

This section presents the results of the simulations. Based on the simulations carried out, three REZ transmission lines are most frequently overloaded: lines 28, 32, and 43. Figures 8–10 show a comparison between the loading level of each line when storage systems are included and the loading level of each line when storage systems are not included.

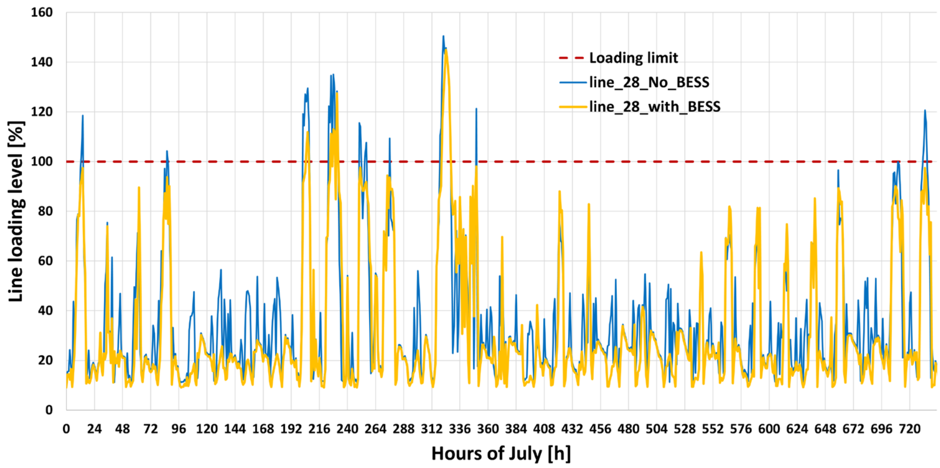

Figure 8. Loading level of line 28.

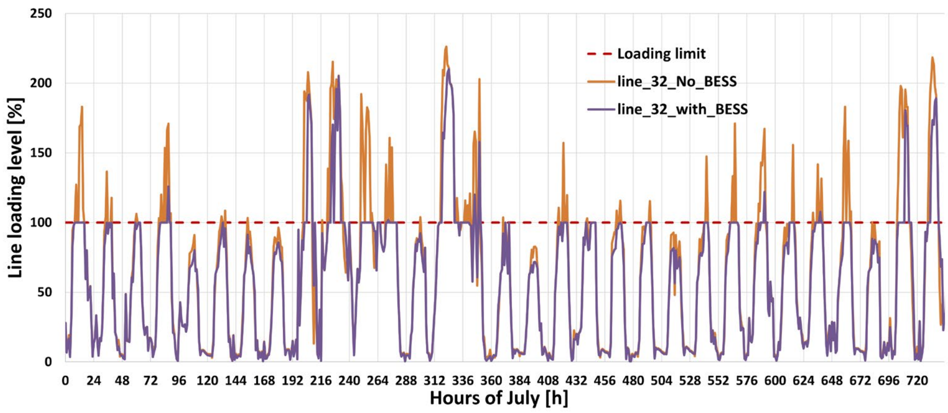

Figure 9. Loading level of line 32.

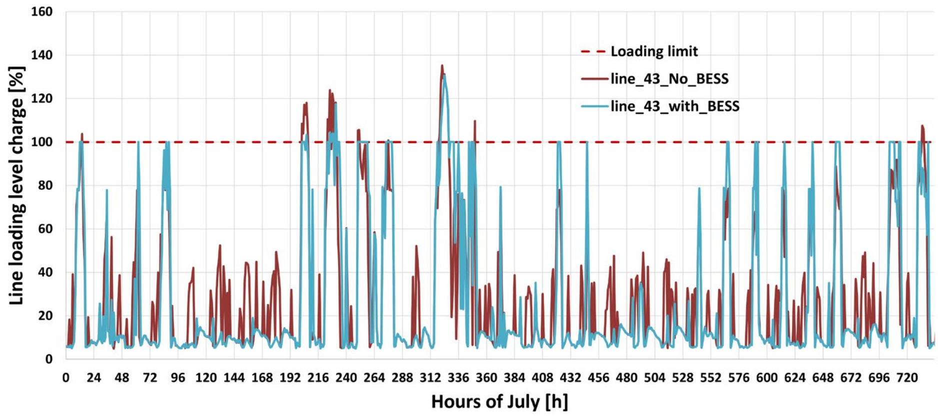

Figure 10. Loading level of line 43.

Looking at Figures 8–10, several important observations can be made. First, storage systems are effectively activated to absorb energy precisely when at least one of the REZ lines has reached its charge limit. Without the use of storage systems in these moments, at least one line would be overloaded. Thanks to the chosen target function, this does not happen, except when the storage systems are saturated or their $E_{max,i}$ is insufficient.

Figure 11 shows the typical behavior of a storage system according to the activation logic proposed in the methodology. When storage is not needed, it remains discharged. It accumulates when necessary to avoid congestion and discharges the stored energy as soon as possible, without causing congestion but maximizing the use of transmission lines to export energy through external grids.

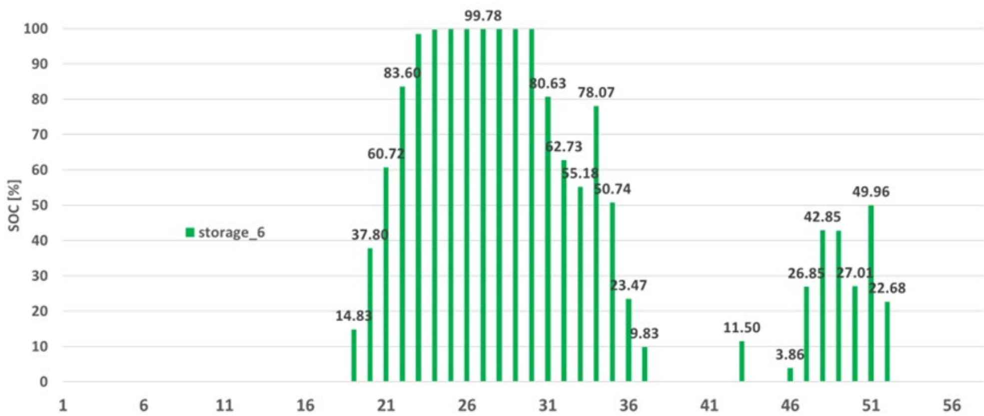

Figure 11. SOC of storage number six during certain hours of the simulation period.

Another important consideration can be made by observing Figure 9, which shows line 32 loading level. During the hours with the greatest gap between generation and load, line 32 is the first to reaches its charge limit and requires the BESS to absorb energy. In the same hours, lines 28 and 43 often are overloaded, but less so than line 32. This depends on two factors: ampacity of the transmission lines and topology of the REZ. Line 32 operates at 220 kV and has a significantly higher ampacity than lines 28 and 43, which operate at 150 kV. Despite this, line 32 remains the bottleneck of the REZ.

Figure 12 shows the location of these lines within the REZ. The network topology and the location of the generation plants cause line 32 to play a key role in exporting the energy produced in the REZ.

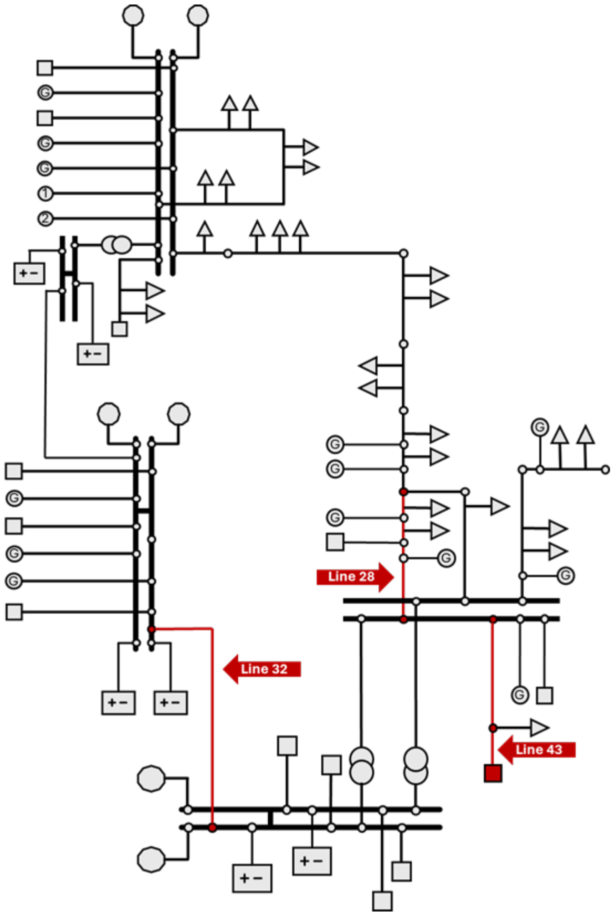

Figure 12. Overloaded lines position within the REZ.

Based on Equation (9) shown in the methodology, the values of LO_{28}, LO_{32}, and LO_{43} were calculated for the three lines that presented significant overloads. Based on Equation (10), the value of LO_{tot} was also calculated, and the results are shown in Figure 13. The results are clear: the use of storage systems as modeled is highly effective in mitigating grid congestion in the network analyzed in the case study. Thanks to storage systems, approximately 13 GWh of grid congestion could be avoided in a typical future summer month. Figure 13 also shows that LO_{32} is significantly higher than LO_{28} and LO_{43}. This result is consistent with the analysis of the loading level of the lines previously observed in Figures 8–10. Another important result is the utilization rate of the six proposed storage systems throughout the period. Figure 14 shows the storage systems and how they have been named. Figure 15 shows the percentile distribution of energy absorbed by storage systems over the entire period analyzed. Storage systems 5 and 6 absorbed at least 16 MWh in 6% of the hours in July. It can be deduced that storage systems 5 and 6 are the most frequently operated storages and play the most important role in limiting grid congestion by maximizing energy export outside the REZ. In 3% of the hours in July, storage systems operated at their maximum design capacity. This means that although storage systems sized with a value of $E_{max,i}$ equal to 50 MWh were effective in avoiding most congestion, larger storage capacities would have been more effective in some hours.

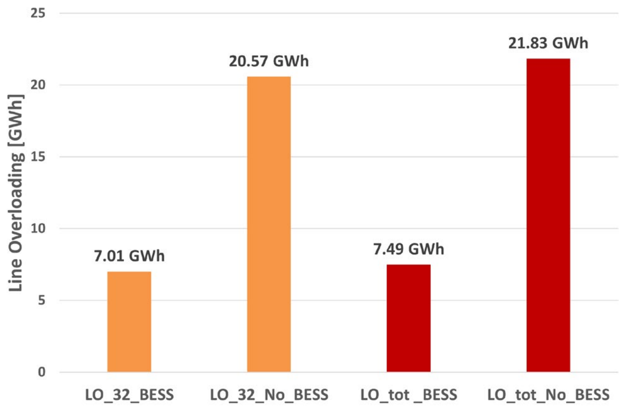

Figure 13. Line overloading in a typical future summer month.

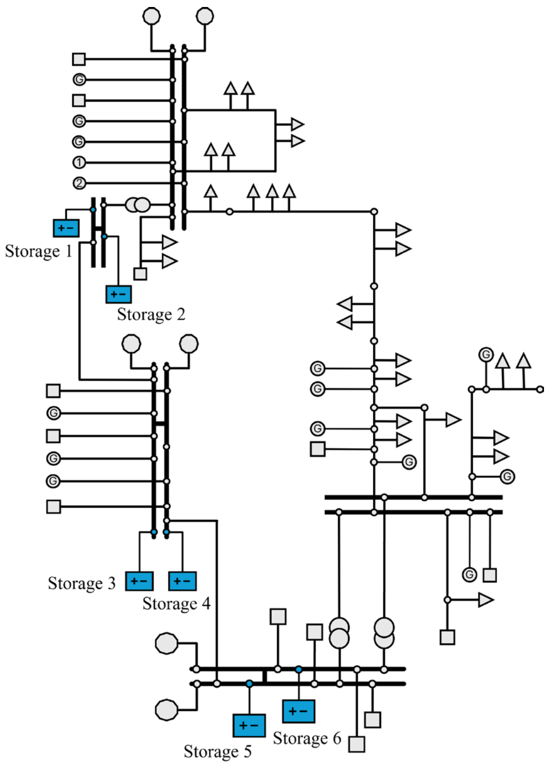

Figure 14. Nomenclature of storage systems.

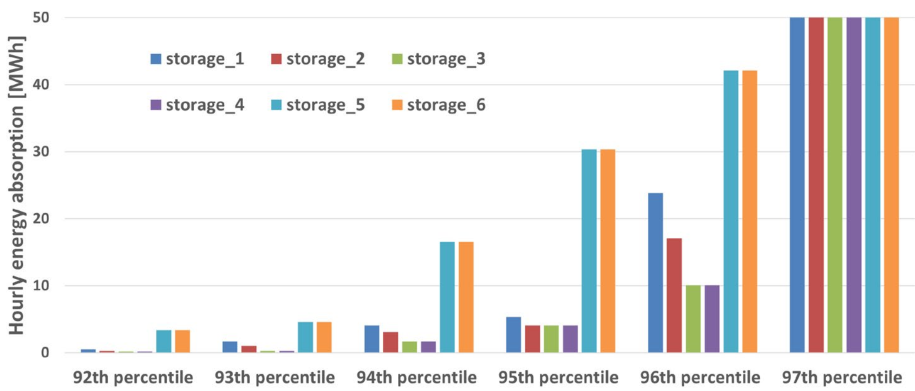

Figure 15. Percentile distribution of hourly energy absorption of storages.

Another noteworthy result concerns the SOC trend of each storage device. Figure 16 shows the SOC percentile distribution of the storages. On average, the most heavily loaded units are storage 5 and storage 6, which are confirmed to be the most important for the network. These are fully saturated for 3% of the hours in the simulation period, making some congestion unavoidable. The value of $C_{max,i}$ chosen corresponds to 330 MWh when considering the charging limit (below 80%) and discharging limit (above 20%) required to preserve battery lifetime. Based on the results obtained, it may be possible to resize the storage capacity of each storage unit to optimize its use.

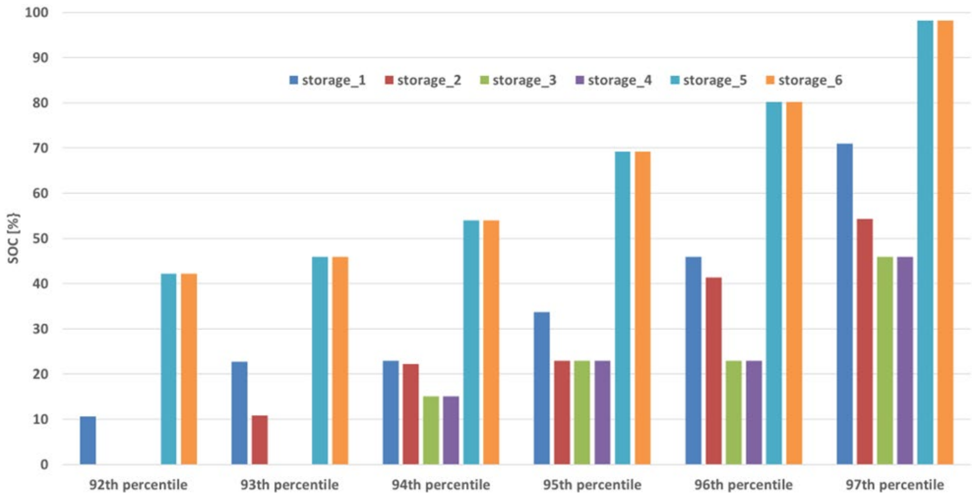

Figure 16. SOC percentile distribution of storages.

6. Conclusions

This paper presents a methodology for testing the size and the location of BESSs in power transmission grids. The model was developed in Python using the open-source Pandapower library. The proposed time-series optimal power flow model includes detailed operational constraints, namely state of charge limits, round-trip efficiency, self-discharge behavior, and ramp rate restrictions.

The validation of the network model, carried out by comparing it with real data obtained from the TDV company software, demonstrated a high degree of consistency between the simulated results and the measured flows. The results indicate that the network has been correctly modeled in the Python environment and that the OPF logic used by the PP library is consistent with that used in practice by the Italian TSO.

The case study results clearly show the effectiveness of BESS in mitigating congestion, avoiding up to 13 GWh grid congestion in a typical future summer month, and optimizing the export of renewable energy produced in the REZ. The parameters used to size the storage systems in Table 4 have proven to be fully effective in mitigating network congestion. Nevertheless, a further increase in the size of some BESSs could provide additional benefits.

The proposed methodology stands out for its ease of implementation, use of free and accessible tools, adaptability to different network scenarios and for the use of an innovative approach: Renewable Energy Zones behave as equivalent generators for the rest of the electrical system, so the OPF calculation is based on this assumption. It therefore represents a useful decision-support tool for network operators and for planning electrical infrastructure in contexts with high penetration of renewable sources. The study also outlines several potential directions for future work. The lack of an economic assessment is also noteworthy. This aspect could certainly have an impact, but it was decided not to address it and it could be a future development of the work.

The analysis could also be extended to a longer time horizon, such as a whole year. A methodology could be developed to automate the identification of the optimal characteristics and siting of BESSs. The complementary use of other technologies such as Dynamic Thermal Rating [6,31,32] or High Temperature Low Sag conductors [33] could be investigated. Last, in order to verify the results obtained in this study, the simulations could be repeated on different REZs with different topologies.

Author Contributions: Conceptualization, F.M. (Fabio Massaro), F.M. (Francesco Montana) and N.C.; methodology, N.C. and S.P.; validation, N.C., F.M. (Fabio Massaro) and F.M. (Francesco Montana); resources, S.P. and E.D.M.; data curation, N.C. and S.P.; writing—original draft preparation, N.C., F.M. (Francesco Montana) and S.P.; supervision, E.D.M. and F.M. (Fabio Massaro); project administration, E.D.M. All authors have read and agreed to the published version of the manuscript.

Funding: This research received no external funding.

Institutional Review Board Statement: Not applicable.

Informed Consent Statement: Not applicable.

Data Availability Statement: The data used are confidential.

Conflicts of Interest: The authors declare no conflicts of interest.

Abbreviations

The following abbreviations are used in this manuscript:

BESS	Battery Energy Storage Systems
MACSE	Meccanismo di Approvvigionamento di Capacità di Stoccaggio Elettrico
OPF	Optimal Power Flow
PF	Power Flow
PNIEC	Piano Nazionale Integrato per l'Energia e il Clima
PP	Pandapower
RES	Renewable Energy Sources
REZ	Renewable Energy Zone
TDV	Terna Data Viewer
TSO	Transmission System Operator

References

1. Terna, S.p.A. *Stato del Sistema Elettrico e Scenari Energetici*; Terna S.p.A: Rome, Italy, 2025. Available online: https://download.terna.it/terna/Terna_Piano_Sviluppo_2025_Stato_sistema_elettrico_scenari_energetici_8dd62ec4bbb9f75.pdf (accessed on 16 May 2025).
2. Musca, R.; Sanseverino, E.R.; Vasile, A.; Zizzo, G.; Iaria, A.; L'Abbate, A.; Vitulano, L. Power-Flow studies on the Future Electricity Grid of Sicily: Analysis of 2030 Scenario Cases. In Proceedings of the 2023 AEIT International Annual Conference (AEIT), Tokyo, Japan, 6–8 January 2023; pp. 1–6. [CrossRef]
3. Favuzza, S.; Ippolito, M.G.; Massaro, F.; Mineo, L.; Musca, R.; Zizzo, G. New energy corridors in the euro-mediterranean area: The pivotal role of Sicily. *Energies* **2018**, *11*, 1415. [CrossRef]
4. Ministero dello Sviluppo Economico Italiano. *PIANO NAZIONALE INTEGRATO PER L'ENERGIA E IL CLIMA*; Ministero dello Sviluppo Economico Italiano: Rome, Italy, 2019. Available online: https://www.mase.gov.it/sites/default/files/archivio/pniec_finale_17012020.pdf (accessed on 16 May 2025).
5. Terna, S.p.A. *Esigenze di Sviluppo: I Nuovi Progetti*; Terna S.p.A: Rome, Italy, 2025. Available online: https://download.terna.it/terna/Terna_Piano_Sviluppo_2025_Esigenze_sviluppo_nuovi_progetti_8dd62eca67348ba.pdf (accessed on 16 May 2025).
6. Massaro, F.; Collura, N.; Paradiso, S.; Di Gloria, P.; Vergine, C. Dynamic Thermal Rating and Development of Renewable Energy Zones in Sicily. *Appl. Sci.* **2025**, *15*, 1987. [CrossRef]
7. Lee, N.; Flores-Espino, F.; Hurlbut, D.J. *Renewable Energy Zone (REZ) Transmission Planning Process: A Guidebook for Practitioners*; National Renewable Energy Laboratory: Golden, CO, USA, 2017. [CrossRef]
8. Terna, S.p.A. *Piano di Sviluppo 2025—Overview*; Terna S.p.A: Rome, Italy, 2025. Available online: https://download.terna.it/terna/Terna_Piano_Sviluppo_2025_Overview_8dd62ebfc87edf6.pdf (accessed on 16 May 2025).

9. Khalili, S.; Lopez, G.; Breyer, C. Role and trends of flexibility options in 100% renewable energy system analyses towards the Power-to-X Economy. *Renew. Sustain. Energy Rev.* **2025**, *212*, 115383. [CrossRef]
10. Lawder, M.T.; Suthar, B.; Northrop, P.W.; De, S.; Hoff, C.M.; Leitermann, O.; Crow, M.L.; Santhanagopalan, S.; Subramanian, V.R. Battery energy storage system (BESS) and battery management system (BMS) for grid-scale applications. *Proc. IEEE* **2014**, *102*, 1014–1030. [CrossRef]
11. Chatzigeorgiou, N.G.; Theocharides, S.; Makrides, G.; Georghiou, G.E. A review on battery energy storage systems: Applications, developments, and research trends of hybrid installations in the end-user sector. *J. Energy Storage* **2024**, *86*, 111192. [CrossRef]
12. Hutters, C.H.; Ruiz, P.; de Boer, S. Battery Energy Storage Systems in Europe. RaboResearch. 2025. Available online: https://www.rabobank.com/knowledge/linkto/d011473382-backup-power-for-europe-part-3-italy-s-bet-on-bess (accessed on 26 August 2025).
13. CRITERI E CONDIZIONI PER IL FUNZIONAMENTO DEL SISTEMA DI APPROVVIGIONAMENTO A TERMINE DI CAPACITÀ DI STOCCAGGIO ELETTRICO. Rome. 2023. Available online: https://www.arera.it/fileadmin/allegati/docs/23/247-23.pdf (accessed on 24 September 2025).
14. Terna, S.p.A. *Documento di Descrizione Degli Scenari 2024*; Terna S.p.A: Rome, Italy, 2024. Available online: https://download.terna.it/terna/Documento_Descrizione_Scenari_2024_8dce2430d44d101.pdf (accessed on 16 May 2025).
15. Chen, X.; Du, F.; Cao, Y.; Tan, Z.; Yan, Z. Inertia Ancillary Service Market Mechanism for Renewable-Dominated Power Systems: A Review. In Proceedings of the 2025 IEEE International Conference on Power and Integrated Energy Systems (ICPIES), Haikou, China, 7–9 April 2025; pp. 618–623. [CrossRef]
16. Di Carlo, S.; Genna, A.; Massaro, F.; Montana, F.; Sanseverino, E.R. Optimizing Renewable Power Management in Transmission Congestion. An Energy Hub Model Using Hydrogen Storage. In Proceedings of the 21st IEEE International Conference on Environment and Electrical Engineering and 2021 5th IEEE Industrial and Commercial Power System Europe, EEEIC/I and CPS Europe, Bari, Italy, 7–10 September 2021. [CrossRef]
17. Sekhar, S.C.; Sharma, V.K. Analysis of Power System Dynamics with Renewable Integration and Battery Storage for a 3 bus ring connected system. In Proceedings of the 2024 IEEE Pune Section International Conference, PuneCon 2024, Pune, India, 13–15 December 2024. [CrossRef]
18. Thurner, L.; Scheidler, A.; Schäfer, F.; Menke, J.H.; Dollichon, J.; Meier, F.; Meinecke, S.; Braun, M. Pandapower—An Open-Source Python Tool for Convenient Modeling, Analysis, and Optimization of Electric Power Systems. *IEEE Trans. Power Syst.* **2018**, *33*, 6510–6521. [CrossRef]
19. Bolgaryn, R.; Banerjee, G.; Meinecke, S.; Maschke, H.; Marten, F.; Richter, M.; Liu, Z.; Lytaev, P.; Alfakhouri, B.; Kisse, J.; et al. Open Source Simulation Software pandapower and pandapipes: Recent Developments. In Proceedings of the 2023 Open Source Modelling and Simulation of Energy Systems (OSMSES), Aachen, Germany, 27–29 March 2023. Available online: https://www.digsilent.de/en/powerfactory.html (accessed on 16 May 2025).
20. Bolgaryn, R.; Banerjee, G.; Cronbach, D.; Drauz, S.; Liu, Z.; Majidi, M.; Maschke, H.; Wang, Z.; Thurner, L. Recent Developments in Open Source Simulation Software pandapower and pandapipes. In Proceedings of the 2022 Open Source Modelling and Simulation of Energy Systems (OSMSES), Aachen, Germany, 4–5 April 2022; pp. 1–7. [CrossRef]
21. Nababan, B.P.; Sutrisna, K.F.; Pratama, M.; Nainggolan, S.W. Influence of battery energy storage system on system stability in isolated power system. In Proceedings of the ICT-PEP 2021—International Conference on Technology and Policy in Energy and Electric Power: Emerging Energy Sustainability, Smart Grid, and Microgrid Technologies for Future Power System, Jakarta, Indonesia, 29–30 September 2021; pp. 22–27. [CrossRef]
22. Malmström, T.; Sterner, E. A Framework Development for Battery Energy Storage System Siting Using Data-Driven Insights. Master's Thesis, Uppsala University, Uppsala, Sweden, 2025.
23. Liu, Z.; Majidi, M.; Wang, H.; Mende, D.; Braun, M. Time Series Optimization-Based Characteristic Curve Calculation for Local Reactive Power Control Using Pandapower-PowerModels Interface. *Energies* **2023**, *16*, 4385. [CrossRef]
24. Klimov, A.; Matrenin, P. Electric Network Topology Optimization with Distributed Generation using Pandapower Library. *J. Mod. Energy Res.* **2024**, *2*, 1–6. [CrossRef]
25. Terna. STUDIO SULLE TECNOLOGIE DI RIFERIMENTO PER LO STOCCAGGIO DI ENERGIA ELETTRICA. Rome. 2023. Available online: https://www.google.com/url?sa=t&rct=j&q=&esrc=s&source=web&cd=&ved=2ahUKEwihoYe00daSAxWwpJUCHTlhBuMQFnoECCIQAQ&url=https://download.terna.it/terna/Studio_tecnologie_di_accumulo_8db9511fbdd7601.pdf&usg=AOvVaw2ObR50gi5-U1to16y9eIhq&opi=89978449 (accessed on 13 February 2026).
26. Ippolito, M.G.; Massaro, F.; Cassaro, C. HTLS Conductors: A Way to Optimize RES Generation and to Improve the Competitiveness of the Electrical Market—A Case Study in Sicily. *J. Electr. Comput. Eng.* **2018**, *2018*, 2073187. [CrossRef]
27. Di Gloria, P.; Paradiso, S.; Pede, M.; Sorrentino, V.M.E.; Vergine, C.; Massaro, F.; Vasile, A.; Zizzo, G. On the Impact of Renewable Generation on the Sicilian Power System in Near-Future Scenarios: A Case Study. *Energies* **2024**, *17*, 3352. [CrossRef]

28. Collura, N.; Massaro, F.; Di Mambro, E.; Paradiso, S.; Montana, F.; Buscemi, A. Optimization of a Battery Energy Storage System in a Sicilian Renewable Energy Zone. In Proceedings of the 2025 IEEE International Conference on Environment and Electrical Engineering and 2025 IEEE Industrial and Commercial Power Systems Europe (EEEIC/I&CPS Europe), Chania, Greece, 15–18 July 2025.
29. Kim, S.H.; Shin, Y.J. Optimize the operating range for improving the cycle life of battery energy storage systems under uncertainty by managing the depth of discharge. *J. Energy Storage* **2023**, *73*, 109144. [CrossRef]
30. Tomaszewska, A.; Chu, Z.; Feng, X.; O'kane, S.; Liu, X.; Chen, J.; Ji, C.; Endler, E.; Li, R.; Liu, L.; et al. Lithium-ion battery fast charging: A review. *eTransportation* **2019**, *1*, 100011. [CrossRef]
31. Karimi, S.; Musilek, P.; Knight, A.M. Dynamic thermal rating of transmission lines: A review. *Renew. Sustain. Energy Rev.* **2018**, *91*, 600–612. [CrossRef]
32. Lai, C.-M.; Teh, J. Comprehensive review of the dynamic thermal rating system for sustainable electrical power systems. *Energy Rep.* **2022**, *8*, 3263–3288. [CrossRef]
33. Riba, J.-R.; Bogarra, S.; Gómez-Pau, Á.; Moreno-Eguilaz, M. Uprating of transmission lines by means of HTLS conductors for a sustainable growth: Challenges, opportunities, and research needs. *Renew. Sustain. Energy Rev.* **2020**, *134*, 110334. [CrossRef]

https://doi.org/10.3390/electricity7020035